Hindawi
Advances in Materials Science and Engineering
Volume 2018, Article ID 3897348, 10 pages
https://doi.org/10.1155/2018/3897348

Research Article

Models for Strength Prediction of High-Porosity Cast-In-Situ Foamed Concrete

Wenhui Zhao,[1,2] **Junjie Huang**,[1,2] **Qian Su**,[1,2] **and Ting Liu**[1,2]

[1]*School of Civil Engineering, Southwest Jiaotong University, Chengdu, China*
[2]*MOE Key Laboratory of High-Speed Railway Engineering, Southwest Jiaotong University, Chengdu, China*

Correspondence should be addressed to Junjie Huang; jjhuang_swjtu@126.com

Received 30 October 2017; Revised 4 February 2018; Accepted 7 March 2018; Published 26 April 2018

Academic Editor: João M. P. Q. Delgado

A study was undertaken to develop a prediction model of compressive strength for three types of high-porosity cast-in-situ foamed concrete (cement mix, cement-fly ash mix, and cement-sand mix) with dry densities of less than 700 kg/m^3. The model is an extension of Balshin's model and takes into account the hydration ratio of the raw materials, in which the water/cement ratio was a constant for the entire construction period for a certain casting density. The results show that the measured porosity is slightly lower than the theoretical porosity due to few inaccessible pores. The compressive strength increases exponentially with the increase in the ratio of the dry density to the solid density and increases with the curing time following the composite function $A_2(\ln t)^{B_2}$ for all three types of foamed concrete. Based on the results that the compressive strength changes with the porosity and the curing time, a prediction model taking into account the mix constitution, curing time, and porosity is developed. A simple prediction model is put forward when no experimental data are available.

1. Introduction

Foamed concrete is an important type of geotechnical material [1]. It is a light solidification material mainly composed of cement, a filler, and a percentage of stable tiny bubbles and possesses the advantages of being light weight, vertically stable, and convenient for construction [2–5]. The statistical results compiled by the China Concrete and Cement Products Association (CCPA) indicate that the annual production volume of foamed concrete was over 40 million·m^3 in China in 2016, of which more than 80% was cast-in-situ foamed concrete. Due to the increase in large-scale construction and civil engineering projects, the applications of foamed concrete will increase in the future. Therefore, it is important to control the quality of foamed concrete. In the application of foamed concrete for engineering projects, the quality indicators are the casting density during the casting process and the compressive strength during the design stage. However, it is important to know the compressive strength of the foamed concrete at different times after the casting process and during the initial construction period. Therefore, it is necessary to develop a compressive strength prediction model by considering the important parameters and the mix compositions. The strength of foamed concrete is influenced by a number of parameters that have been determined in previous studies [6–8]. The uniaxial compressive strength is given by

$$\sigma = f\left(\sigma_0, p, m, \frac{m_w}{m_c}, \ldots\right), \tag{1}$$

where σ_0 is the uniaxial compressive strength of concrete at a porosity of 0; p is the porosity; m is the degree of hydration, $0 \le m \le 1$, $m = 0$ means the start of the hydration and $m = 1$ means the completion of the hydration; and m_w/m_c is the water/cement ratio.

Based on (1), for the same curing conditions and mix composition, the strength of the foamed concrete is mainly influenced by the porosity, the degree of hydration, and the water/cement ratio. Several models have been proposed to express this ratio, and they are listed in Table 1. It is evident that several compressive strength prediction models for foamed concrete are based on the Powers model and the

Table 1: Review of compressive strength prediction models for foamed concrete.

Author	Material composition	Models
Balshin [8]	Cement	$\sigma = \sigma_0 (1-p)^n$
Neville [9]	Cement, sand, fly ash	$\sigma = kg^n$
Tam et al. [10]	Cement	$\sigma = k(1/(1+m_w/m_c+m_a/m_c))^n$
Durack and Weiqing [11] Nambiar and Ramamurthy [12]	Cement, sand, fly ash	$\sigma = k((2.06\alpha V_c)/(1-V_{fl}-V_c(1-\alpha)))^n$
Hoff [13]	Cement	$\sigma = \sigma_0((d_c(1+0.2\rho_c))/((1+k_s)\rho_c\gamma_w))^b$
Kearsley and Wainwright [14]	Cement, sand, fly ash	$\sigma = \sigma_0((d_c(1+0.2\rho_c+s_v))/((1+k_s)(1+s_w)\rho_c\gamma_w))^b$

σ = the uniaxial compressive strength of foamed concrete; p = porosity; g = gel-space ratio; m_a/m_c = the air/cement ratio; d_c = casting density; ρ_c = the specific gravity of cement; γ_w = unit weight of water; k_s = water-solid ratio by weight; σ_0 = uniaxial compressive strength of concrete at a porosity of 0; s_w = filler-cement ratio by weight; s_v = admixture-cement ratio by volume; k = gel strength; α = hydration water-cement ratio by weight; V_c = volume of cement; V_{fl} = filler volume of unit volume; d_c = fresh density; b, n = empirical constant.

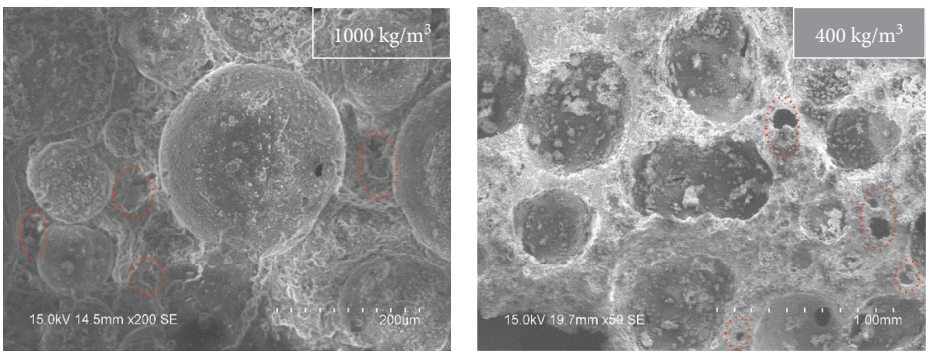

(a) (b)

Figure 1: Comparison of voids in (a) high-density and (b) low-density casting of foamed concrete. Red dotted circles: small voids in the pore walls.

Balshin model; most prediction models have limitations in terms of the influencing factors of porosity, the degree of hydration, and the water/cement ratio.

As can be seen in Figure 1, foamed concrete is a typical noncompacting type of concrete; therefore, the porosity of foamed concrete is controlled by the volume of the voids in the concrete. The voids include gel pores, microcapillaries, macrocapillaries, and artificial air pores [15, 16]. Based on (1), its compressive strength is related to the proportion occupied by voids. Odler and Röβler [7] established a relationship between porosity and strength for a series of cement pastes with different water/cement ratios after periods of hydration. The research showed that the relationship between the compressive strength and the porosity is linear for porosity values between 5% and 28%. Fagerlund [17] stated that it is necessary to determine a limit for the porosity. When the porosity is below the limit, an equation fits the experimental data. For higher porosities, a different equation is required. As the foamed concrete density increases, the pore spaces become smaller and the pore walls become thicker. When the dry density of foamed concrete is more than 700 kg/m^3 (the relative density is about 0.3), there is a transitional change and the material changes from a porous structure to a solid structure containing isolated pores [18]. The dry density of foamed concrete used as roof insulation material ranges from 160 to 300 kg/m^3. For heat insulation material, the dry density ranges from 300 to 500 kg/m^3. When used as geotechnical fill material, its dry density ranges from 400 to 600 kg/m^3 [19, 20]. As we can see, all values all smaller than 700 kg/m^3.

For a given casting density of foamed concrete, when the water/cement ratio is low, the added bubbles will burst while the mixture is being stirred and the flow requirement of the foamed concrete cannot be reached. When the water/cement ratio is high, instability will occur for the fresh foamed concrete and the bubbles float on top of the foamed concrete slurry. This separation phenomenon between the foam and the cement slurry influences the casting results [21, 22]. These two phenomena related to bubble instability are shown in Figure 2. For the cast-in-situ foamed concrete during construction, the flow value is regulated between 160 and 180 mm. As for the cast-in-situ foamed concrete, a superplasticizer was not added during the production process due to limitations in the construction conditions and the construction equipment; therefore, the water/cement ratio was a constant value for a given casting density.

The degree of hydration of the foamed concrete is a function of time, curing temperature, and other parameters. As the curing time increases, the cement hydration in the foamed concrete may produce solid products that fill the pores of the sample. At the same time, the self-weight consolidation and evaporation of water may significantly increase the stiffness and density of the samples [23]. A study on the effect of the relationship between water permeability and pore connectivity under different curing times indicated that the sample had a coarse structure during the early stage,

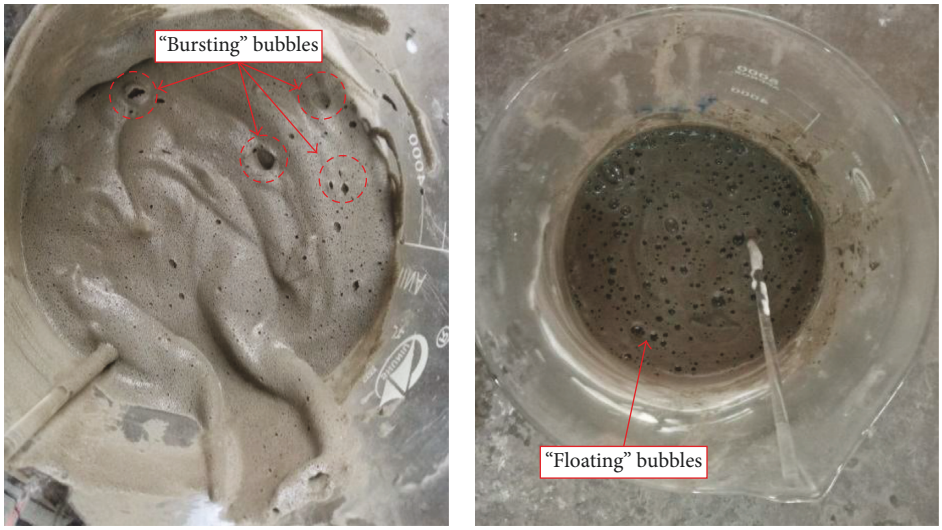

(a) (b)

Figure 2: Bubble instability phenomena: (a) bubble bursting; (b) bubble floating.

Table 2: The constituent materials of the foamed concrete.

Materials	Remarks
Cement	Type I Portland cement conforming to GB 175-2007
Sand	Finer than 300 microns, specific gravity = 2.5
Fly ash	Class F Type I conforming to GB/T 1596-2005
Foaming agent	Synthetic type, specific gravity = 1.06
Water	Tap water

whereas the pore structure in the hardened cement paste became denser as the curing time increased [24, 25]. For the same casting density and curing conditions, the compressive strength of foamed concrete varies with the curing time; therefore, it is necessary to know the compressive strength for different curing times.

In view of these observations, it is necessary to develop a model for compressive strength prediction of high-porosity cast-in-situ foamed concrete that should consider the porosity and the degree of hydration. The model can help determine the mix composition of the foamed concrete, the casting density, and the compressive strength. At the same time, it will provide a reference for the initial construction time of the engineering project.

2. Materials and Methods

2.1. Materials. The foamed concrete used in this study was made from ordinary Portland cement, fine sand, fly ash, and bubbles. The constituent materials used in the experiments are shown in Table 2. In this research, a synthetic type of foaming agent was used because it was highly eco-friendly and its air bubbles were strong. The bubbles were entrained or entrapped within the slurry to promote lightness [26, 27].

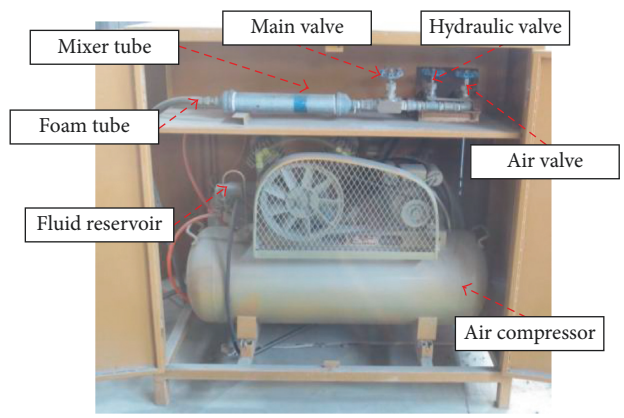

Figure 3: Air bubble generator.

2.2. Mix Design Procedure. To produce the bubbles for the production of the samples, the foaming agent was diluted with water at a ratio of 1 : 60 (namely, the multiple of dilution equals 60). A prefoaming method was used to produce the foamed concrete. In this method, the air bubbles were first foamed by a bubble generator, which is shown in Figure 3. The density of air bubbles was set at $35 \pm 5\,\mathrm{kg/m^3}$.

A flowchart of the foamed concrete mix method is shown in Figure 4. The cement, fly ash, and sand were mixed with water at a certain ratio to produce a cement slurry as shown in Table 3. After that, the air bubbles were mixed well with the cement slurry by stirring with an electric blender to produce the foamed concrete.

2.3. Samples and Maintenance Procedure. Twenty-one densities of foamed concrete were cast; the corresponding mix proportions and major parameters are listed in Table 3. For each density, the number of groups was decided by the testing time. Six identical samples (100 mm long × 100 mm wide × 100 mm high) were prepared for each group and

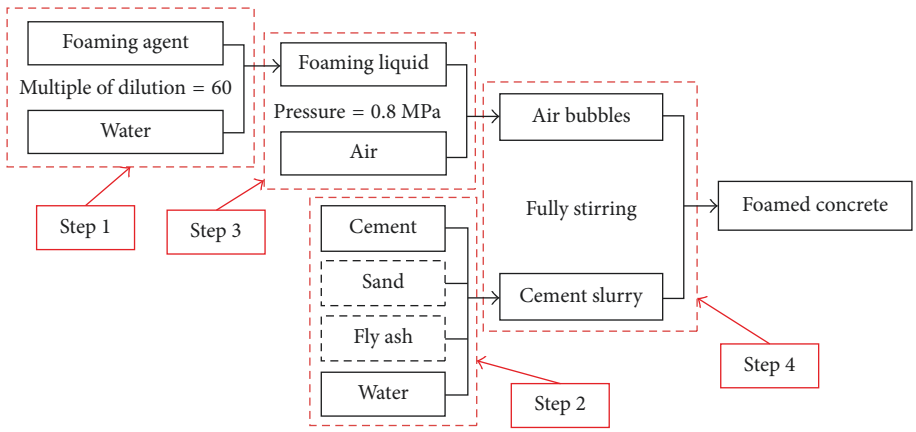

Figure 4: Flowchart of the foamed concrete mix method [28].

testing time. Three samples were used to test the compressive strength, and the others were used to measure the dry densities. The samples were demoulded after 24 h to ensure that they were sufficiently hard for further handling. Then, all the test samples were subjected to standard curing.

2.4. Testing Method

2.4.1. Compressive Strength. The cubes were tested by using a compressive machine at the pace rates of 2.00 kN/s according to the "Test method of autoclaved aerated concrete" (GBT 11969-2008). The stress data were recorded to determine the unconfined compressive strength. The data used for the analysis consisted of the average of three sample test results.

2.4.2. Porosity. The measured porosity of the foamed concrete was determined using a vacuum saturation apparatus. The samples were placed in an electric, constant-temperature drying oven at 60°C for 24 h. After that, the temperature was increased to 80°C and maintained for 24 h. The samples were dried at 100°C until the weight of the samples was constant. After the samples were placed into the vacuum saturation apparatus (Figure 5), the pressure was maintained at −1 MPa for 2 h. After turning on the air valve, water flowed into the device slowly until the samples were immersed in the liquid. Prior to the weighing tests, the samples were saturated for another 22 h. The measured porosity was calculated using the following formula [29]:

$$P = \frac{(W_{sat} - W_{dry})}{(W_{sat} - W_{wat})} \times 100, \quad (2)$$

where P is the vacuum saturation porosity (%), W_{sat} is the weight in air of the saturated sample, W_{wat} is the weight in water of the saturated sample, and W_{dry} is the weight of oven-dried sample.

3. Results and Discussion

Nambiar and Ramamurthy [12, 30] expressed the theoretical porosity of foamed concrete using the variables of casting density, water-solid ratio, filler-cement ratio of the freshly foamed concrete mixture, specific gravity of the cement, and unit weight of water, which can be seen in (3) and (4). According to previously determined data, the porosity values vary from 0.18 to 0.23 for different kinds of raw materials and different proportions of ingredients [10, 31, 32]. The ratio of hydration water to cement by weight is assumed to be 0.2.

$$n = 1 - \frac{d_c(1 + 0.2\rho_c)}{(1 + k_s)\rho_c\gamma_w}, \quad (3)$$

$$n = 1 - \frac{d_c(1 + 0.2\rho_c + s_v)}{(1 + k_s)(1 + s_w)\rho_c\gamma_w}. \quad (4)$$

These equations are inconvenient and flawed. First of all, there are many variables that need to be calculated. Secondly, it is assumed that the hydration of the cement is complete, which ignores the degree of cement hydration. Lastly, these equations do not consider the difference in the hydration water between the cement and the admixtures. In order to avoid these problems, the following equation can be used to determine the theoretical porosity [18]:

$$n = 1 - \frac{\rho^*}{\rho_s}, \quad (5)$$

where ρ^* is the dry density of foamed concrete and ρ_s is the dry density of the solid material.

In (5), the dry density can be considered a certain value for the same mix constitution for the same brand of material when it is completely hydrated. When the constitution proportions of the materials change, ρ_s can be obtained based on the proportions of the constitutions. The hydrations of the cement and admixtures are functions of the curing time, and the degree of hydration will affect the dry density. When the hydration is complete and the testing time is long enough, (3) and (4) are applicable. However, (5) applies in all cases. In addition, this equation is simple and intuitive.

The relationship between the measured and theoretical porosities (after 1 year) of foamed concrete is shown in Figure 6. It is evident that deviations exist between the measured and theoretical porosities. For all mixes, the

Table 3: Mix proportions and major parameters of foamed concrete.

Mix number	$m_c + m_m + m_s$	f/c	s/c	w/binder	Water (kg)	Cement (kg)	Fly ash (kg)	Sand (kg)	Air bubbles (l)	Dry density (kg/m^3)	Casting density (kg/m^3)	Flow value (cm)	Testing time (d)
1		0	0	0.75	173.0	230.7	0.0	0.0	752.6	291.3	430.1	16.1	7, 28, 90, 180, 270, 365
2	A	0	1 : 1	0.63	144.2	115.4	0.0	115.4	772.5	255.8	401.9	17.7	7, 28, 90, 180, 270, 365
3		1 : 1	0	0.75	173.0	115.4	115.4	0.0	745.4	274.5	429.8	16.8	7, 28, 90, 180, 270, 365
4		0	0	0.70	204.5	292.2	0.0	0.0	701.2	367.3	521.3	16.2	28, 365
5	B	0	1 : 1	0.59	172.4	146.1	0.0	146.1	722.0	324.8	489.9	16.5	28, 365
6		1 : 1	0	0.70	204.5	146.1	146.1	0.0	692.1	345.4	521.0	16.9	28, 365
7		0	0	0.65	229.9	353.7	0.0	0.0	656.0	427.6	606.6	16.5	28, 365
8	C	0	1 : 1	0.56	196.4	176.9	0.0	176.9	675.8	391.8	573.8	16.6	28, 365
9		1 : 1	0	0.65	229.9	176.9	176.9	0.0	645.0	421.3	606.2	17.2	28, 365
10		0	0	0.60	249.1	415.2	0.0	0.0	616.9	514.9	685.9	16.8	7, 28, 90, 180, 270, 365
11	D	0	1 : 1	0.52	215.9	207.6	0.0	207.6	634.1	461.5	653.3	17.5	7, 28, 90, 180, 270, 365
12		1 : 1	0	0.60	249.1	207.6	207.6	0.0	604.1	496.2	685.5	17.4	7, 28, 90, 180, 270, 365
13		0	0	0.55	262.2	476.7	0.0	0.0	584.0	585.4	759.3	16.8	28, 365
14	E	0	1 : 1	0.49	233.6	238.4	0.0	238.4	594.1	526.4	731.2	17.1	28, 365
15		1 : 1	0	0.55	262.2	238.4	238.4	0.0	569.3	561.2	758.8	17.7	28, 365
16		0	0	0.54	290.6	538.2	0.0	0.0	535.8	645.6	847.6	17.1	28, 365
17	F	0	1 : 1	0.48	258.3	269.1	0.0	269.1	547.2	597.2	815.7	16.8	28, 365
18		1 : 1	0	0.54	290.6	269.1	269.1	0.0	519.1	638.1	847.0	17.6	28, 365
19		0	0	0.53	317.8	599.7	0.0	0.0	488.7	705.4	934.6	16.7	7, 28, 90, 180, 270, 365
20	G	0	1 : 1	0.47	281.9	299.9	0.0	299.9	501.5	663.8	899.1	17.5	7, 28, 90, 180, 270, 365
21		1 : 1	0	0.53	317.8	299.9	299.9	0.0	470.1	687	934.0	17.4	7, 28, 90, 180, 270, 365

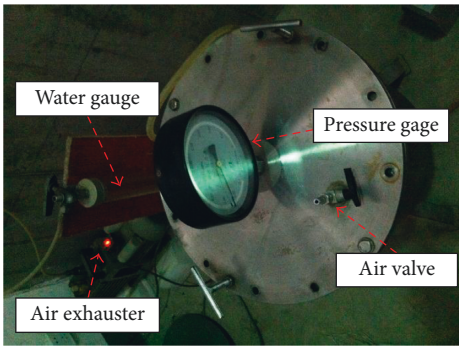

Figure 5: Vacuum saturation device.

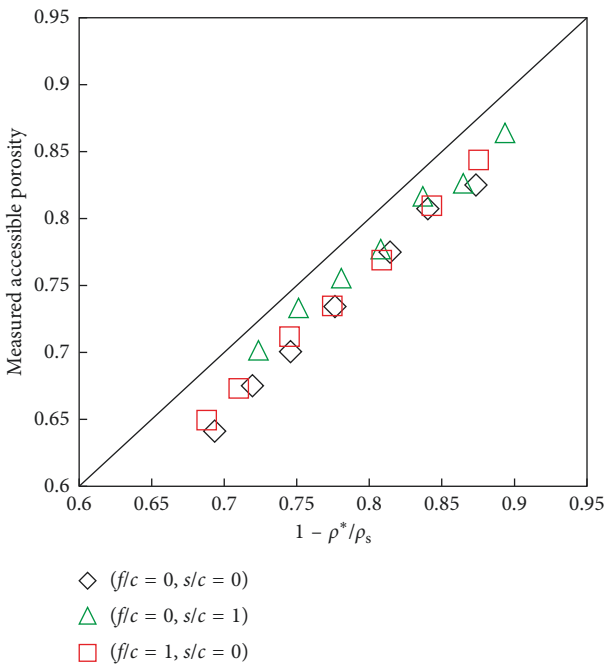

Figure 6: Relationship between measured porosity and $1-\rho^*/\rho_s$.

measured values are lower than the theoretical values. The reason is that foamed concrete has closed pores, which are difficult to fill entirely with water. The closed pores differ for different casting densities. In high-density casting, the closed pores occur in the pore structures and pore walls, while in low-density casting, the closed pores mainly occur in the pore walls. A comparison of the differences between the measured and theoretical porosities for the three types of foamed concrete of the same casting density indicates that the difference is largest for the cement mix, followed by the cement-fly ash mix and the cement-sand. After the addition of fly ash, the initial setting time of the foamed concrete increases resulting in instability of the foamed concrete slurry and an increase in the number of connected holes [14]. For the foamed concrete containing sand, the pore walls become thinner and the number of the connected holes increases due to the reduction in the cement proportion and the increase in the density of the solid material [33, 34]. When the number of connected holes increases, there is a higher likelihood that the voids are filled with water, which decreases the deviations between the measured and the theoretical porosities.

3.1. Effect of Porosity on Compressive Strength. The relationship between the theoretical porosity and the compressive strength (28 days and 1 year) of the foamed concrete is shown in Figure 7. The data show that the compressive strength increases exponentially with the increase in ρ^*/ρ_s as described in (6); this occurs for all types of foamed concrete for the 1 yr duration and the 28 d duration.

$$\sigma = A_1\left(\frac{\rho^*}{\rho_s}\right)^{B_1}. \tag{6}$$

A comparison between Figures 7(a) and 7(b) shows that the dry density is slightly higher for 1 yr than for 28 d for the same density of foamed concrete because the hydration reaction is not fully complete at 28 d, which is consistent with previously reported results [2]. For the three conditions ($f/c=0$, $s/c=0$; $f/c=0$, $s/c=1$; $f/c=1$, $s/c=0$), the A_1 value is higher for 1 yr than for 28 d. The B_1 value is lowest for the cement-sand mix, followed by the cement mix and the cement-fly ash mix.

Table 4 lists the constants of the strength-porosity models of the foamed concrete with various mix constituents. It shows that the values of the constants obtained in this study are close to the values obtained by Hoff [13] using cement paste. However, the constants obtained in this study are lower than those obtained by Nambiar and Ramamurthy [12] for cement-sand. Nambiar and Ramamurthy [21] stated that foamed concrete with a fly ash additive was less dependent on the pore parameters than foamed concrete with sand; these results differ from our results. Figure 8 shows the microscopic photographs of the pore wall structures of the foamed concrete with different casting densities. The pore wall structure is dense for the high-density casting and less dense for the low-density casting. In the low-porosity foamed concrete ($f/c=0$, $s/c=1$), the sand has an interlocking effect under pressure. In the high-porosity foamed concrete ($f/c=0$, $s/c=1$), the hole walls are thinner and less dense, which reduces the interlocking effect. Therefore, in this study, the σ_0 parameter of high-porosity foamed concrete only reflects the uniaxial compressive strength of the mix constitution.

3.2. Effect of Curing Time on Compressive Strength. Most of the existing compressive strength prediction models have been used to predict the strength of the foamed concrete after casting at particular times, while the compressive strength of foamed concrete increases with the curing time. Because the use of the foamed concrete begins at 28 d after casting or earlier, it is important to predict the strength of foamed concrete immediately after casting and thereafter.

The effects of the curing time on the compressive strengths of three casting densities are shown in Figure 9. It can be seen that the compressive strength increases with the

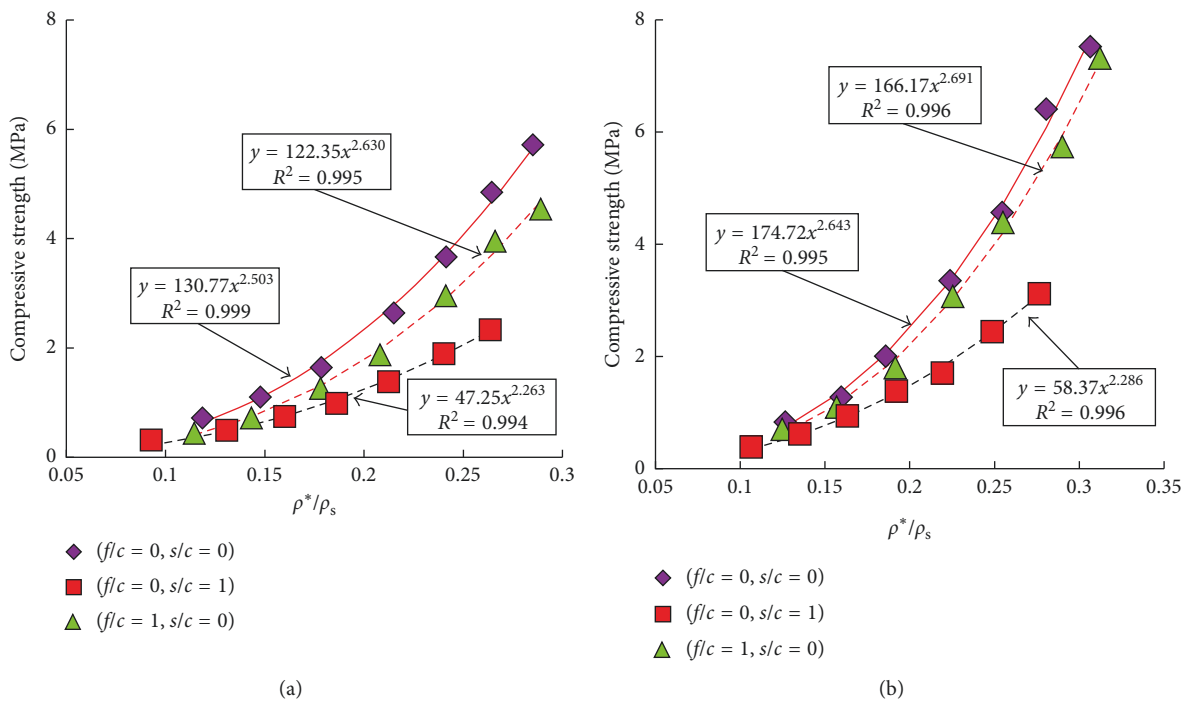

Figure 7: Effect of porosity on compressive strength at (a) 28 days and (b) 1 year.

Table 4: Comparison of the constants of various strength-porosity models.

Model by	Mix constituents	Constants	
		σ_0	b
Hoff [13]	Cement	115–290	2.7–3
Kearsley and Wainwright [14]	Cement with and without fly ash	188	3.1
Nambiar and Ramamurthy [12]	Cement-sand	155.66	4.3
	Cement-sand-fly ash	105.14	2.58
Present study	Cement	174.72	2.643
	Cement-sand	58.37	2.286
	Cement-fly ash	166.17	2.691

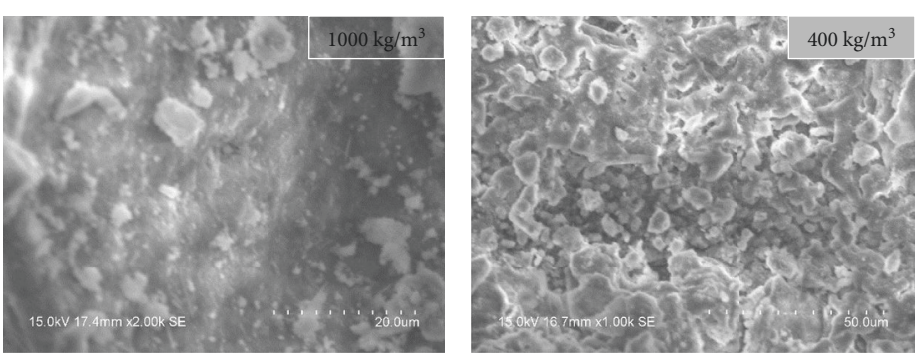

(a) (b)

Figure 8: Microscopic photographs of the pore wall structures of (a) high-density and (b) low-density casting foamed concrete.

curing time; initially, the rate of increase in the compressive strength is large and it slows as the curing time increases. The relationship between the compressive strength and the curing time can be expressed by the following equation for a given density and mix constitution:

$$\sigma = A_2 (\ln t)^{B_2}. \quad (7)$$

A comparison of the results shown in Figures 9(a)–9(c) indicates that for the same casting density and curing time, the compressive strength is highest for the cement mix, followed by

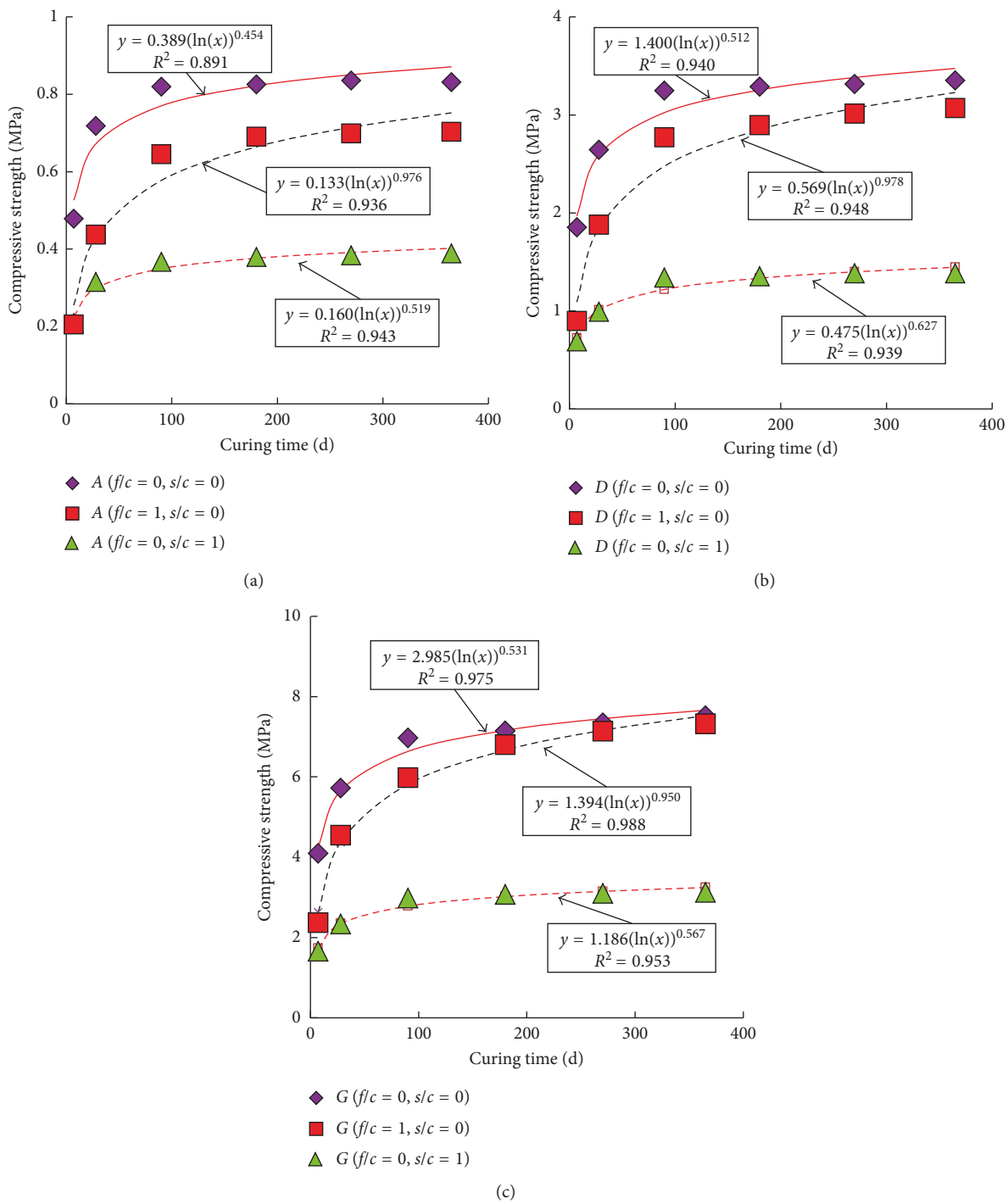

Figure 9: Effect of curing time on compressive strength for the three casting densities: (a) A, (b) D, and (c) G.

the cement-fly ash mix and the cement-sand mix. The compressive strength is almost stable at 90 d for the cement mix and the cement-sand mix; the compressive strength does not increase after 180 d for the cement-fly ash mix. It is evident that the values provided by the prediction model are lower during the early stage and higher during the late stage compared with the test values. The compressive strength decreases when fly ash is added, but the attenuation ratio decreases with an increase in the casting density. The B_2 values are similar for the cement mix and the cement-sand mix, but the B_2 value is lower for the cement-fly ash mix. Because the hydration reaction material in the cement mix and the cement-sand mix is cement, the hydration rates are very similar under the same curing conditions [35], while the hydration rate of the fly ash is lower. The B_2 value represents the hydration rate of the raw material.

3.3. Proposed Model. Based on the above results, the compressive strength of foamed concrete is a function of the mix

Table 5: Comparison of the constants of various mix constituents.

Mix constituents	A	B	C	$A(\ln 365)^B$	R^2
Cement	110.255	0.204	2.568	158.362	0.997
Cement-sand	34.989	0.305	2.292	60.123	0.995
Cement-fly ash	59.551	0.531	2.603	152.830	0.993

Table 6: Comparison of the constants of various mix constituents ($\rho^* = \rho^*_{365}$).

Mix constituents	A	B	C	$A(\ln 365)^B$	R^2
Cement	60.640	0.470	2.459	139.655	0.988
Cement-sand	22.771	0.518	2.244	57.106	0.991
Cement-fly ash	33.315	0.821	2.548	143.055	0.982

constitution, curing time, and porosity. The following equation is derived from (6) and (7):

$$\sigma = A(\ln t)^B \left(\frac{\rho^*}{\rho_s}\right)^C, \tag{8}$$

where t is the curing time, $1 < t \leq 365$; A is the parameter associated with the compressive strength of concrete; B is the parameter reflecting the hydration rate of the mix constituents; and C is the parameter reflecting the porosity and pore structure, which is associated with the pore quality including pore size, pore shape, and so on.

When (8) is used to fit the test data, ρ^* is measured when the compressive strength is tested. Table 5 shows the constants of various mix constituents. It can be inferred that there is no obvious difference in the B value for cement and cement-sand, whereas the B value of the cement-fly ash is high, which is in agreement with the foregoing conclusions. Compared with the B values shown in Figure 9, the values are lower in Table 5 because the hydration rate of the mix constituent is reflected by the parameters B and C. When parameter C is added to the equation, the value of B decreases.

The parameter ρ^* is rarely measured outside the laboratory when a strength prediction model is used. It is important to reduce the number of measurements. The dry densities are similar for different curing times for the same casting densities. When the differences are ignored, the dry densities are only measured after 1 yr. The results are shown in Table 6.

A comparison of the data shown in Tables 5 and 6 shows that the A and C values are lower in Table 6 for the same mix constitutions, while the B values are higher. The degree of fit decreases for all mix constitution, although a high degree of fit is still ensured. Therefore, the assumption of $\rho^* = \rho^*_{365}$ is reasonable in order to simplify the model. At the same time, ρ^* can be simply calculated using (9) according to the "Technical specification for application of foamed concrete" (JGJT341-2014):

$$\rho^* = S_a(m_c + m_m) + m_s, \tag{9}$$

where S_a is an empirical constant for certain cement and admixture factories, m_c is the cement dosage of foamed concrete per cubic meter, m_m is the admixture dosage of foamed concrete per cubic meter, and m_s is the fine aggregate dosage of foamed concrete per cubic meter.

In this study, S_a equals to 1.211, 1.216, and 1.175 for the cement mix, cement-sand mix, and cement-fly ash mix, respectively. The values are very similar for the cement mix and the cement-sand mix. The value is slightly lower for the cement-fly ash mix because cement is a hydraulic binding material and fly ash is the active mineral admixture; the addition of fly ash reduces the value of S_a. Cement is the hydration reaction material in the cement-sand mix, and sand is the nonactive admixture; therefore, the S_a values are similar for the cement mix and the cement-sand mix. Combined with the other results, (9) can be used to calculate the dry density, in which S_a is an empirical constant for a given mix constitution and a given cement factory. When there are no measurements of dry density, the following equation can be used to predict the compressive strength of foamed concrete:

$$\sigma = A(\ln t)^B \left(\frac{S_a(m_c + m_m) + m_s}{\rho_s}\right)^C. \tag{10}$$

4. Conclusion

The following conclusions can be drawn based on the experimental and comparative results:

(1) The measured porosity is slightly lower than the theoretical porosity due to few inaccessible pores.

(2) The compressive strength increases with the increase in the ratio of dry density to solid density following the equation $A_1(\rho^*/\rho_s)^{B_1}$ for all three types of foamed concrete. The B_1 value is similar for the cement mix and the cement-fly ash mix. The value of B_1 is lowest for the cement-sand mix, followed by the cement mix and the cement-fly ash mix.

(3) The compressive strength increases with the curing time following the composite function $A_2(\ln t)^{B_2}$ for all three types of foamed concrete. The B_2 values are similar for the cement mix and cement-sand mix, but the B_2 value is lower for the cement-fly ash mix.

(4) Based on the results that the compressive strength changes with the porosity and the curing time, a prediction model taking into account the mix constitution, curing time, and porosity is proposed. A simple prediction model is put forward when no experimental data are available.

Conflicts of Interest

The authors declare that there are no conflicts of interest regarding the publication of this paper.

Acknowledgments

This work was supported by the Sichuan Science and Technology Support Project (2016JY0005) and the China Railway Science and Technology Research Plan Project (2015G002-K).

References

[1] C. Hu, H. Li, Z. Liu, and Q. Wang, "Research on properties of foamed concrete reinforced with small sized glazed hollow beads," *Advances in Materials Science and Engineering*, vol. 2016, Article ID 5820870, 8 pages, 2016.

[2] K. Ramamurthy, E. K. K. Nambiar, and G. I. S. Ranjani, "A classification of studies on properties of foam concrete," *Cement and Concrete Composites*, vol. 31, no. 6, pp. 388–396, 2009.

[3] Z. Liu, K. Zhao, C. Hu, and Y.-F. Tang, "Effect of water-cement ratio on pore structure and strength of foam concrete," *Advances in Materials Science and Engineering*, vol. 2016, Article ID 9520294, 9 pages, 2016.

[4] P. Onprom, K. Chaimoon, and R. Cheerarot, "Influence of bottom ash replacements as fine aggregate on the property of cellular concrete with various foam contents," *Advances in Materials Science and Engineering*, vol. 2015, Article ID 381704, 11 pages, 2015.

[5] Y. S. Jeong and H. K. Jung, "Thermal performance analysis of reinforced concrete floor structure with radiant floor heating system in apartment housing," *Advances in Materials Science and Engineering*, vol. 2015, Article ID 367632, 7 pages, 2015.

[6] M. Röβler and I. Odler, "Investigations on the relationship between porosity, structure and strength of hydrated Portland cement pastes I. Effect of porosity," *Cement and Concrete Research*, vol. 15, no. 2, pp. 320–330, 1985.

[7] I. Odler and M. Röβler, "Investigations on the relationship between porosity, structure and strength of hydrated Portland cement pastes. II. Effect of pore structure and of degree of hydration," *Cement and Concrete Research*, vol. 15, no. 3, pp. 401–410, 1985.

[8] M. Y. Balshin, "Relation of mechanical properties of powder metals and their porosity and the ultimate properties of porous metal-ceramic materials," *Doklady Akademii Nauk SSSR*, vol. 67, no. 5, pp. 831–834, 1949.

[9] A. Neville, *Properties of Concrete*, Wiley, New York, NY, USA, 1996.

[10] C. T. Tam, T. Y. Lim, R. Sri Ravindrarajah, and S. L. Lee, "Relationship between strength and volumetric composition of moist-cured cellular concrete," *Magazine of Concrete Research*, vol. 39, no. 138, pp. 12–18, 1987.

[11] J. M. Durack and L. Weiqing, "The properties of foamed air cured fly ash based concrete for masonry production," in *Proceedings of the Fifth Australasian Masonry Conference*, Gladstone, QLD, Australia, July 1998.

[12] E. K. K Nambiar and K. Ramamurthy, "Models for strength prediction of foam concrete," *Materials and Structures*, vol. 41, no. 2, pp. 247–254, 2008.

[13] G. C. Hoff, "Porosity-strength considerations for cellular concrete," *Cement and Concrete Research*, vol. 2, no. 1, pp. 91–100, 1972.

[14] E. P. Kearsley and P. J. Wainwright, "The effect of high fly ash content on the compressive strength of foamed concrete," *Cement and Concrete Research*, vol. 31, no. 1, pp. 105–112, 2001.

[15] A. A. Hilal, N. H. Thom, and A. R. Dawson, "On entrained pore size distribution of foamed concrete," *Construction and Building Materials*, vol. 75, pp. 227–233, 2015.

[16] Z. Pan, H. Li, and W. Liu, "Preparation and characterization of super low density foamed concrete from Portland cement and admixtures," *Construction and Building Materials*, vol. 72, pp. 256–261, 2014.

[17] G. Fagerlund, "Strength and porosity of concrete," in *Proceedings of the International Symposium on Pore Structure and Properties of Materials (RILEM/IUPAC)*, pp. 51–141, Prague, Czech Republic, September 1973.

[18] L. J. Gibson and M. F. Ashby, *Cellular Solids: Structure and Properties*, Cambridge University Press, Cambridge, UK, 1999.

[19] X. Tan, W. Chen, Y. Hao, and X. Wang, "Experimental study of ultralight (<300 kg/m^3) foamed concrete," *Advances in Materials Science and Engineering*, vol. 2014, Article ID 514759, 7 pages, 2014.

[20] B. Dolton and C. Hannah, "Cellular concrete: Engineering and technological advancement for construction in cold climates," in *Proceedings of the 2006 Annual General Conference of the Canadian Society for Civil Engineering*, Calgary, AB, Canada, May 2006.

[21] E. K. K. Nambiar and K. Ramamurthy, "Fresh state characteristics of foam concrete," *Journal of Materials in Civil Engineering*, vol. 20, no. 2, pp. 111–117, 2008.

[22] M. R. Jones, K. Ozlutas, and L. Zheng, "Stability and instability of foamed concrete," *Magazine of Concrete Research*, vol. 68, no. 11, pp. 542–549, 2016.

[23] E. K. K. Nambiar and K. Ramamurthy, "Sorption characteristics of foam concrete," *Cement and Concrete Research*, vol. 37, no. 9, pp. 1341–1347, 2007.

[24] K. Kurumisawa and K. Tanaka, "Three-dimensional visualization of pore structure in hardened cement paste by the gallium intrusion technique," *Cement and Concrete Research*, vol. 36, no. 2, pp. 330–336, 2006.

[25] T. H. Wee, S. B. Daneti, and T. Tamilselvan, "Effect of w/c ratio on air-void system of foamed concrete and their influence on mechanical properties," *Magazine of Concrete Research*, vol. 63, no. 8, pp. 583–595, 2011.

[26] E. Kuzielová, L. Pach, and M. Palou, "Effect of activated foaming agent on the foam concrete properties," *Construction and Building Materials*, vol. 125, pp. 998–1004, 2016.

[27] D. K. Panesar, "Cellular concrete properties and the effect of synthetic and protein foaming agents," *Construction and Building Materials*, vol. 44, pp. 575–584, 2013.

[28] W. H. Zhao, Q. Su, T. Liu, and J. J. Huang, "Experimental study on the frost resistance of cast-in-situ foamed concrete," *Electronic Journal of Geotechnical Engineering*, vol. 22, pp. 5509–5523, 2017.

[29] J. G. Cabrera and C. J. Lynsdale, "A new gas permeameter for measuring the permeability of mortar and concrete," *Magazine of Concrete Research*, vol. 40, no. 144, pp. 177–182, 1988.

[30] E. P. Kearsley and P. J. Wainwright, "The effect of porosity on the strength of foamed concrete," *Cement and Concrete Composites*, vol. 32, no. 2, pp. 233–239, 2002.

[31] H. F. W. Taylor, *Cement Chemistry*, Thomas Telford Ltd., London, UK, 1997.

[32] P. Hewlett, *Lea's Chemistry of Cement and Concrete*, Butterworth-Heinemann, Oxford, UK, 2003.

[33] E. K. K. Nambiar and K. Ramamurthy, "Models relating mixture composition to the density and strength of foam concrete using response surface methodology," *Cement and Concrete Composites*, vol. 28, no. 9, pp. 752–760, 2006.

[34] F. Batool and V. Bindiganavile, "Air-void size distribution of cement based foam and its effect on thermal conductivity," *Construction and Building Materials*, vol. 149, pp. 17–28, 2017.

[35] E. K. K. Nambiar and K. Ramamurthy, "Influence of filler type on the properties of foam concrete," *Cement and Concrete Composites*, vol. 28, no. 5, pp. 475–480, 2006.